Using In-Home Energy Storage to Improve the Resilience of Residential Electricity Supply

Rachel Hunter-Rinderle, Matthew Y. Fong, Baihua Yang, Haoshu Xian, and Ramteen Sioshansi *Fellow, IEEE*

Electricity-supply interruptions can be costly and disruptive. Electricity-supply reliability and resilience can be enhanced by customers having on-site energy storage, which supplements electricity-system supply. This paper proposes a two-stage stochastic optimization model that can be used in a rolling-horizon fashion to schedule such use of energy storage. We demonstrate the model with a case study that combines electricity-supply-reliability data for a real-world electric utility, survey data regarding residential customers' willingnesses to pay for backup energy during electricity-supply disruptions, and a highly resolved Markov chain model of building-occupant behavior and associated electricity use that is calibrated to census data. We find that the low probability of an electricity-supply disruption occurring during any given time-step limits the charging of the energy storage in anticipation of possible disruptions. We demonstrate two approaches to reduce this myopic use of energy storage. Our case study shows that penalty parameters can be used to control the conservatism of the model in using as opposed to retaining stored energy during an electricity-supply disruption. Overall, we show the viability of on-site energy storage to enhance electricity-supply reliability and resilience and the feasibility of our model and algorithm for real-time control of energy storage for such a real-world application.

***Index Terms*—Energy storage, electricity-system reliability, stochastic optimization**

NOMENCLATURE

Sets and Indices

a	activity index
$\mathcal{A}$	activity set
t	time index
$\mathcal{T}$	ordered set, $\mathcal{T} = \{t_{\text{st}}, \ldots, t_{\text{en}}\}$, of time periods of the optimization horizon
ω	index of scenarios
Ω	set of scenarios

Parameters

$C_{\omega,t}$	retail electricity price during time t of scenario ω (\$/kWh)
$D_{\omega,t,a}$	activity-a power demand during time t of scenario ω (kW)
$\bar{E}$	energy capacity of energy storage (kWh)
E_{st}	starting state of energy (SOE) of energy storage (kWh)
$\bar{P}$	power capacity of energy storage (kW)
Δ	time-step duration (h)
η	round-trip efficiency of energy storage (p.u.)
$\kappa_{\omega,t,a}$	penalty for curtailing activity-a energy demand during time t of scenario ω (\$/kWh)
π_ω	probability of scenario ω occurring
$\sigma_{\omega,t}$	equals 1 if electricity-system supply is available during time t of scenario ω and equals 0 otherwise

Variables

$E_{\omega,t}$	beginning time-t SOE of energy storage under scenario ω (kWh)
$s^E_{\omega,t,a}$	energy-storage-supplied power to serve activity a during time t of scenario ω (kW)
$s^G_{\omega,t,a}$	electricity-system-supplied power to serve activity a during time t of scenario ω (kW)
$\iota_{\omega,t}$	power charged into energy storage during time t of scenario ω (kW)

This work was supported by National Science Foundation grants 1463492, 1808169and 1922666, Carnegie Mellon Electricity Industry Center, and a grant of computational resources from The Ohio State University's Department of Integrated Systems Engineering. *(Corresponding author: R. Sioshansi.)*

R. Hunter-Rinderle is with Department of Integrated Systems Engineering, The Ohio State University, Columbus, OH 43210-1271, USA (e-mail: hunter-rinderle.2@buckeyemail.osu.edu).

M. Y. Fong is with Department of Computer Science Engineering, The Ohio State University, Columbus, OH 43210-1277, USA (e-mail: fong.131@buckeyemail.osu.edu).

B. Yang is with Thomas Lord Department of Computer Science, University of Southern California, Los Angeles, CA 90089-0134, USA (e-mail: baihuaya@usc.edu).

H. Xian is with Department of Industrial and Operations Engineering, University of Michigan, Ann Arbor, MI 48109-2117, USA (e-mail: haoshu@umich.edu).

R. Sioshansi is with Department of Engineering and Public Policy, Carnegie Mellon Electricity Industry Center, Department of Electrical and Computer Engineering, and Wilton E. Scott Institute for Energy Innovation, Carnegie Mellon University, Pittsburgh, PA 15213-3815, USA and with Department of Integrated Systems Engineering, The Ohio State University, Columbus, OH 43210-1271, USA (e-mail: rsioshan@andrew.cmu.edu).

I. INTRODUCTION

ELECTRICITY-SUPPLY resilience is a growing concern for customers, regulators, and policymakers. For example, an electricity-supply disruption in Texas during February 2021 claimed at least 111 lives and had a disproportionate impact on socioeconomically vulnerable populations [1]. An analysis by LaCommare and Eto [2] estimates that electricity-supply disruptions in United States of America (US) impose an annual national social cost of \$30 billion–\$130 billion. Another analysis finds that the utility sector having a 1% inoperability rate could yield an annual expected GDP loss of \$11.6 billion, measured with 2019 dollars [3].

One approach to mitigate the impact of electricity-supply disruptions is through infrastructure investment and hardening [4]. This approach depends upon having proper regulatory structures to incentivize long-term planning by electricity-sector actors [5]. Another approach, which is our focus, is

to use distributed energy storage to provide end customers with energy that supplements bulk-electricity-system supply [6]. The extant literature that examines such uses of energy storage can be divided into two categories [7].

One set of works [8]–[29] examines the impact of energy storage on bulk-electricity-system reliability. These works take different approaches to estimate or approximate the impact of energy storage on electricity-system reliability [30], [31]. One approach uses planning-reserve margins [8]–[10]. A second approach uses probabilistic or analytic methods [32], whereby the impact of energy storage on the likelihood of an electricity-system reliability event is estimated directly [11]–[14]. A third option is to employ Monte Carlo simulation [15]–[20]. Among other factors, this literature shows that operational representation and information revelation [21], [22], the resource mix [10], [23]–[26], load patterns [12], and resource hybridization [27], [28] impacts this use of energy storage.

A second body of work [33]–[39] examines the use of energy storage by individual or groups of consumers to manage electricity-supply disruptions. These works differ in analytical scope. Some works consider energy storage alone [33]–[36], hybridized energy storage [37], [38], or energy storage that is part of a system with multiple energy carriers [39].

These two sets of works differ in their foci *vis-à-vis* reliability and resilience benefits of energy storage. As is common of resource-adequacy modeling, the former [8]–[29] focuses on generator failures and capacity availability on the ability of the bulk electricity system to serve load reliably. The reliability of end-customer electricity service often is impacted by transmission- or distribution-infrastructure failures hindering energy deliverability. Thus, the latter body of work [33]–[39] may focus on different failure mechanisms. Another distinction between these two sets of work is that the latter may examine load prioritization. For instance, during a hot summer day, food refrigeration may be more valuable to a customer than building lighting is. For the most part, reliability analyses of bulk electricity systems do not distinguish the consumer values of different end uses of energy.

This paper adds to the second body of work [33]–[39]. We present a two-stage stochastic optimization model to operate energy storage to mitigate electricity-supply disruptions. We demonstrate the performance of the model using a case study that is calibrated to real-world data. The model uses arbitrary time-steps, which are taken to be ten-minutes-long in our case study. The two-stage structure assumes that the current time-step is stage 1, for which there is no uncertainty. Stage 2 corresponds to the remaining time-steps, during which time electricity supply from the bulk electricity system and electricity demands are uncertain. The model can be used in a rolling-horizon fashion to schedule energy-storage use as uncertainties are revealed.

Our case-study calibration accounts for actual supply-disruption rates for residential customers and the relative value of different energy activities. Our results show a trade-off in energy-storage use that stems from these relative values. If the values of energy activities are relatively different, it is optimal to curtail energy use for low-priority activities during a supply disruption. By doing so, more stored energy is available to serve higher-priority activities during subsequent time-steps (*e.g.*, in the event that an electricity-supply disruption is prolonged). We find that the relatively low probabilities of electricity-supply disruptions yields myopic behavior, whereby the energy storage may not be charged in anticipation of possible disruptions. We examine two approaches to address this undesirable model behavior. In addition, we conduct analyses that demonstrate the sensitivity of energy-storage use to different model and case-study assumptions and parameters.

Taken together, our work makes four primary contributions to the extant literature. The model that we present is computationally efficient and could be used to operate energy storage in this manner in a real-world setting. This potential for real-world use stems from the model being solvable quickly using standard hardware and software that could be deployed in a distributed building energy-management system. Second, we examine the model and energy-storage use with a case study that is calibrated to real-world data, especially residential electricity demands. This can be contrasted with other works that use stylized examples and case studies [33], [35], [37], [38]. Third, we demonstrate two approaches to mitigate myopic model behavior. Finally, we examine the use of penalty parameters to control the conservatism of the model in using as opposed to retaining stored energy during an electricity-supply disruption. To our knowledge, the existing literature neglects these final two issues.

The remainder of this paper is organized as follows. Section II provides our model formulation. Section III summarizes case-study data and calibration and model implementation. Section IV summarizes case-study results and sensitivity analyses. Section V concludes.

II. Optimization Model

Our model is a two-stage stochastic optimization, with an horizon that consists of an ordered set, $\mathcal{T} = \{t_{\mathrm{st}}, \ldots, t_{\mathrm{en}}\}$, of time-steps. The first stage is the first time-step, t_{st}, and the second stage is the remaining time-steps, $t_{\mathrm{st}}+1, \ldots, t_{\mathrm{en}}$. We model a set, Ω, of second-stage scenarios. During each time-step, the building has electricity demands to fulfill a set, $\mathcal{A}$, of different activities. For all $\omega \in \Omega$, $t \in \mathcal{T}$, $a \in \mathcal{A}$, we let $D_{\omega,t,a}$ denote the building's demand for electricity to fulfill activity a during time-step t of scenario ω. For all $\omega \in \Omega$, $t \in \mathcal{T}$, $a \in \mathcal{A}$, if the building's electricity demand for activity a during time-step t of scenario ω is unfulfilled (*e.g.*, during an electricity-supply disruption), there is a p.u. penalty, which is denoted by $\kappa_{\omega,t,a}$. The penalty could reflect an actual cost (*e.g.*, inability to operate a refrigerator causing food spoilage) or an inconvenience (*e.g.*, a building occupant is unable to undertake a desired activity).

The state of the system during stage 1, which is the first time-step, is known and deterministic. This state information includes demand information, $D_{\omega,t_{\mathrm{st}},a}$, $\forall \omega \in \Omega$, $a \in \mathcal{A}$; the starting energy-storage SOE, E_{st}; and the binary parameters, $\sigma_{\omega,t_{\mathrm{st}}}$, $\forall \omega \in \Omega$, which equals 1 if electricity-system supply is available during time-step t_{st} of scenario ω and equals 0 otherwise. Although these data are deterministic, we index them by scenario, which allows us to write and program the

model compactly. The first-stage decisions that the model optimizes are $s^E_{\omega,t_{\rm st},a}$ and $s^G_{\omega,t_{\rm st},a}$, $\forall\omega\in\Omega$, $a\in\mathcal{A}$, which denote the electricity from energy storage and the electricity system, respectively, that is supplied to fulfill activity a during time-step $t_{\rm st}$ of scenario ω and $\iota_{\omega,t_{\rm st}}$, $\forall\omega\in\Omega$, which denotes electricity that is charged into energy storage during time-step $t_{\rm st}$ of scenario ω. These decisions are deterministic, but are indexed by scenario to provide a compact model formulation with non-anticipativity constraints [40].

The remaining stage-2 time-steps, $t_{\rm st}+1,\ldots,t_{\rm en}$, involve the same sets of state information and decision variables. The key difference is that the state information and decisions can vary between scenarios (*i.e.*, there are no non-anticipativity restrictions on the stage-2 decisions). Intuitively, this model structure means that the decisions that are made during time-step $t_{\rm st}$ cannot be based on any knowledge of which scenario occurs. Conversely, decisions that are made during subsequent time-steps can be contingent upon the realized scenario.

Our model formulation is:

$$\min \sum_{\omega\in\Omega,t\in\mathcal{T}} \pi_\omega\Delta\cdot\Bigg\{C_{\omega,t}\iota_{\omega,t}+\sum_{a\in\mathcal{A}}\Big[C_{\omega,t}s^G_{\omega,t,a} + \kappa_{\omega,t,a}\cdot\big(D_{\omega,t,a}-s^E_{\omega,t,a}-s^G_{\omega,t,a}\big)\Big]\Bigg\} \tag{1}$$

$$\text{s.t. } E_{\omega,t+1}=E_{\omega,t}+\Delta\cdot\left(\eta\iota_{\omega,t}-\sum_{a\in\mathcal{A}}s^E_{\omega,t,a}\right);\quad \forall\omega\in\Omega,t\in\mathcal{T} \tag{2}$$

$$s^E_{\omega,t,a}+s^G_{\omega,t,a}\le D_{\omega,t,a};\forall\omega\in\Omega,t\in\mathcal{T},a\in\mathcal{A} \tag{3}$$

$$0\le\iota_{\omega,t}\le\bar{P}\sigma_{\omega,t};\forall\omega\in\Omega,t\in\mathcal{T} \tag{4}$$

$$0\le s^E_{\omega,t,a}\le D_{\omega,t,a};\forall\omega\in\Omega,t\in\mathcal{T},a\in\mathcal{A} \tag{5}$$

$$0\le\sum_{a\in\mathcal{A}}s^E_{\omega,t,a}\le\bar{P};\forall\omega\in\Omega,t\in\mathcal{T} \tag{6}$$

$$0\le s^G_{\omega,t,a}\le D_{\omega,t,a}\sigma_{\omega,t};\forall\omega\in\Omega,t\in\mathcal{T},a\in\mathcal{A} \tag{7}$$

$$0\le E_{\omega,t}\le\bar{E};\forall\omega\in\Omega,t\in\mathcal{T} \tag{8}$$

$$E_{\omega,t_{\rm st}}=E_{\rm st};\forall\omega\in\Omega \tag{9}$$

$$s^G_{\omega,t_{\rm st},a}=s^G_{\omega',t_{\rm st},a};\forall\omega,\omega'\in\Omega,a\in\mathcal{A} \tag{10}$$

$$\iota_{\omega,t_{\rm st}}=\iota_{\omega',t_{\rm st}};\forall\omega,\omega'\in\Omega \tag{11}$$

$$s^E_{\omega,t_{\rm st},a}=s^E_{\omega',t_{\rm st},a};\forall\omega,\omega'\in\Omega,a\in\mathcal{A}. \tag{12}$$

Objective function (1) minimizes expected cost over the optimization horizon, $\mathcal{T}$, and considers two types of costs. The terms, $C_{\omega,t}\iota_{\omega,t}$ and $C_{\omega,t}s^G_{\omega,t,a}$, are the costs of charging the energy storage and serving demands using electricity-system-supplied energy, respectively. The term:

$$\kappa_{\omega,t,a}\cdot\big(D_{\omega,t,a}-s^E_{\omega,t,a}-s^G_{\omega,t,a}\big);$$

is the cost of curtailing electricity demand.

Constraint set (2) is a set of linear energy-balance equalities, which give the evolution of energy-storage SOE from one time-step to the next. Constraint set (3) ensures that energy demands are not oversupplied. Charging limits on energy storage are imposed by (4), which ensure also that no charging occurs during an electricity-supply disruption. Constraint sets (5)–(6) impose per-activity and aggregate limits, respectively, on energy-storage discharging. Constraint set (7) imposes per-activity limits on power that is drawn from the electricity system and ensure that no power is drawn during a supply disruption. Constraint set (8) impose energy limits on the SOE of energy storage.

Non-anticipativity restrictions (9)–(12) encode the two-stage scenario tree that underlies the problem [40]. Specifically, these constraints force all decision variables during stage 1 (*i.e.*, time-step $t_{\rm st}$), to be equal across all of the scenarios. This restriction means that stage-1 decisions cannot depend upon the scenario, ω, that occurs actually. Conversely, all decisions for subsequent time-step can vary across scenarios. Constraint set (9) fixes the starting SOE of the energy storage as of the beginning of the optimization horizon.

III. Case-Study Data, Calibration, and Implementation

We apply our model to a year-long case study that is calibrated using data that correspond to Central Ohio. In particular, we focus on data for Ohio Power Company (AEP Ohio), which is the largest investor-owned electric utility in the study region. Our optimization model assumes a ten-minute time-step duration.

The energy storage is a lithium-ion battery that has a 2.5-kWh energy capacity and a round-trip efficiency of $\eta=0.9801$ and is discharged fully as of the beginning of the case-study year [35]. The battery is connected to a 1.92-kW standard household electric circuit, which gives its charging and discharging capacities. Based on AEP Ohio's residential tariffs in Central Ohio, we assume a \$0.12/kWh retail price for all electricity-system-supplied energy.

A. Rolling-Horizon Algorithm

The case study is implemented by solving (1)–(12) in an iterative fashion one time-step at a time. Algorithm 1 provides pseudocode that outlines the steps of the rolling-horizon process. Line 1 inputs three parameters. E^0 is the starting SOE of the battery as of the beginning of the case study. H is the number of number of time-steps that are modeled, which we take to be 52536 ten-minute time-steps for all but the final day of the modeled year. δ is the time horizon of each optimization model. We study cases with $\delta=144$ and 72, which correspond to 24- and 12-hour optimization horizons, respectively. By comparing these cases we examine the trade-offs between computational cost and the model having greater foresight. Line 2 initializes the algorithm by setting $E_{\rm st}$ equal to E^0 and setting Ξ, which measures actual incurred cost during the modeled year, equal to nil.

Lines 3–9 is the loop, which iterates through each time-step within the case-study horizon. Line 4 updates the starting and ending time-steps of (1)–(12) and 5 updates model data. Details on how π_ω, $\forall\omega\in\Omega$, $\sigma_{\omega,t}$, $\forall\omega\in\Omega,t\in\mathcal{T}$, and $D_{\omega,t,a},\kappa_{\omega,t,a}$, $\forall\omega\in\Omega,t\in\mathcal{T},a\in\mathcal{A}$ are updated are provided in Sections III-D and III-E. Model (1)–(12) is solved on Line 6, the value of Ξ is updated on Line 7, and the starting SOE of the battery for the next time-step is updated on Line 8.

Algorithm 1 Rolling-Horizon Algorithm

input: E^0, H, δ
initialize: $E_{\rm st} \leftarrow E^0$, $\Xi \leftarrow 0$
for $\tau \leftarrow 1$ to H **do**
  $t_{\rm st} \leftarrow \tau$, $t_{\rm en} \leftarrow \tau + \delta$
  update π_ω, $\forall \omega \in \Omega$; $C_{\omega,t}, \sigma_{\omega,t}$, $\forall \omega \in \Omega, t \in \mathcal{T}$; $D_{\omega,t,a}, \kappa_{\omega,t,a}$, $\forall \omega \in \Omega, t \in \mathcal{T}, a \in \mathcal{A}$
  min (1) s.t. (2)–(12)
  $\Xi \leftarrow \Xi + \Delta \cdot \{C_{1,t_{\rm st}} \iota_{1,t_{\rm st}} + \sum_{a \in \mathcal{A}} [C_{1,t_{\rm st}} s^G_{1,t_{\rm st},a} + \kappa_{1,t_{\rm st},a} \cdot (D_{1,t_{\rm st},a} - s^E_{1,t_{\rm st},a} - s^G_{1,t_{\rm st},a})]\}$
  $E_{\rm st} \leftarrow E_{1,t_{\rm st}+1}$
end for

B. Demand Modeling

Power demands are modeled using the approach of Muratori *et al*. [41], which assumes that household electricity demand consists of five components. These components are power that is used by (1) cold appliances (*e.g*., refrigerators), (2) residential lighting, (3) appliances that are in standby mode, (4) appliances that are being used actively, and (5) the heating, ventilation, and air-conditioning (HVAC) system.

We exclude HVAC power demand from our case study, because the requisite battery size to meet these demands would be very high (*e.g*., air-conditioning loads can be very high). Power demands for appliances that are being used are computed by simulating the behavior of the building occupants using a Markov chain, which represents each building occupant as conducting one of eight possible activities during each ten-minute time-step. The eight activities are (1) sleeping, (2) no-power activity (*e.g*., reading), (3) cleaning, (4) laundry, (5) cooking, (6) dishwashing, (7) leisure (*e.g*., watching television), and (8) being away from the building. Sleeping, no-power activity, and being away from the building do not entail any power demand. The power demands of the other activities, which are obtained from the work of Muratori *et al*. [41], are given in Table I. The power demands for cleaning, cooking, and leisure are instantaneous (*e.g*., if a building occupant is cleaning during time-step t and switches to a different activity ten minutes later, the 1250-W demand occurs during time-step t only). Power demands for laundry and dishwashing are continuous (*e.g*., if a building occupant begin dishwashing during time-step t the 1800-W demand is sustained for 90 consecutive minutes while the activity is completed). Cold-appliance demands occur randomly based on typical cycling profiles for residential refrigerators. Lighting and standby-appliance demands do not depend upon building-occupant activities. Standby-appliance demands are constant across time-steps whereas lighting demands differ between daytime and nighttime time-steps.

Because sleeping, no-power activity, and being away from the building do not entail any power demand, we do not include these activities in the set, $\mathcal{A}$. Instead, the set, $\mathcal{A}$, consists of (1) cleaning, (2) laundry, (3) cooking, (4) dishwashing, (5) leisure, (6) cold appliance, (7) standby-appliance, and (8) lighting. We include sleeping, no-power activity, and being away from the building in simulating the Markov chain, as these activities are needed to represent occupant behavior properly. We assume that the *desired* activities of the building occupants (and the associated electricity demands) remain the same if the building does or does not experience an electricity-supply disruption. The Markov chain that is used to simulate building-occupant behavior is calibrated and validated using data from American Time Use Survey and metered residential electricity-demand data [41], [42].

TABLE I
POWER DEMAND OF BUILDING-OCCUPANT ACTIVITIES [41]

Activity	Power Consumption (W)
Cleaning	1250
Laundry	425 (30 minutes) + 3400 (60 minutes)
Cooking	1225
Dishwashing	1800 (90 minutes)
Leisure	200

C. Electricity-System-Outage Modeling

We model electricity-system outages using a discrete-time two-state Markov chain. Assuming that electricity-supply disruptions and restorations are Markovian is reasonable because if failure and restoration times have exponential distributions, the process is memoryless.

Most electric utilities, including AEP Ohio, are required by pertinent regulatory authorities to record and report annual measures of the reliability of electricity service.[1] We make use of three key metrics to calibrate the Markov chain that is used to simulate electricity-system outages. The first is system average interruption frequency index (SAIFI), which is defined as the ratio between the total number of sustained outages that customers experience and the total number of customers that are served. Thus, SAIFI represents the average number of supply disruptions that a customer experiences *per annum*. The second metric is customer average interruption duration index (CAIDI), which is defined as the ratio between the total duration of sustained outages and the total number of sustained outages. Thus, CAIDI represents the average time duration of an electricity-supply disruption. The third metric is system average interruption duration index (SAIDI), which measures the average total amount of time *per annum* that a customer experiences an electricity-supply disruption. By definition, CAIDI is given by SAIDI divided by SAIFI. The electricity industry uses IEEE Standard 1366-2003, which defines a sustained outage as an electricity-supply disruption that is at least five-minutes of duration.

Table II summarizes the reported year-2019 values of these three reliability metrics for AEP Ohio, which we use to calibrate the state-transition probabilities of our Markov chain. Assuming ten-minute time-steps, the probability of transitioning from a non-outage state to an outage state from one time-step to the next is 0.0000228384. The probability of the reserve transition is 0.0705882353.

We validate these probability estimates using Monte Carlo simulation. Specifically, we generate 10000 year-long sample

[1] https://codes.ohio.gov/oac/4901:1-10-10

TABLE II
REPORTED YEAR-2019 RELIABILITY METRICS FOR AEP OHIO

Metric	Value
SAIFI	1.2 outages
CAIDI	140.98 minutes
SAIDI	169.176 minutes

paths of electricity-supply disruptions. The average (among the generated sample paths) amount of time that the system is in an outage state is 170.057 minutes, with a 95% confidence interval of between 165.87 and 174.25 minutes, which contains the reported year-2019 SAIDI value for AEP Ohio. The average number of electricity-supply disruptions among the sample paths is 1.197 and a 95% confidence interval is between 1.18 and 1.22, which contains the reported SAIFI value. Thus, we conclude that the calibrated Markov chain yields the desired statistical properties that are reflected in the reported reliability data.

D. Electricity-Demand-Curtailment Penalties

Lee and Akar [43] describe their use of survey techniques to study the priorities of residential electricity customers and their willingnesses to pay for energy to serve different activities during an electricity-supply disruption. The preliminary survey results are confidential, which limits our ability to share their key findings, which are used in constructing our case study. Specifically, we cannot disclose the relative priorities of different activities (*e.g.*, importance of lighting as opposed to cold appliances). Based on communications with Lee and Akar, we classify the eight energy activities that we model as high- and low-priority activities. We assume that $\forall \omega \in \Omega, t \in \mathcal{T}$, $\kappa_{\omega,t,a} = 1 \times 10^6$ for low-priority activities and consider cases with $\kappa_{\omega,t,a} = 2 \times 10^6$, 5×10^6, and 1×10^7 for high-priority activities $\forall \omega \in \Omega, t \in \mathcal{T}$.

So long as they are sufficiently large, the specific values of $\kappa_{\omega,t,a}$, $\forall \omega \in \Omega, t \in \mathcal{T}, a \in \mathcal{A}$ are unimportant. Rather, the relative scale of these penalties between high- and low-priority activities is important in how stored energy is used during an electricity-supply disruption. If the penalties differ in scale between high- and low-priority activities, stored energy is used for high-priority activities. As such, energy use for low-priority activities is curtailed to retain stored energy for high-priority activities in the event that an electricity-supply disruption has a long duration. This conservative behavior can result in low-priority activities being curtailed unnecessarily during an electricity-supply disruption that is short in duration. Conversely, if all of the penalties are similar in scale, more stored energy will be used to serve low-priority activities. This behavior can result in high-priority activities being curtailed during a long-duration electricity-supply disruption. Comparing cases with different values of $\kappa_{\omega,t,a}$, $\forall \omega \in \Omega, t \in \mathcal{T}$ for high-priority activities allows us to examine these behaviors.

E. Scenario Generation

Line 5 of Algorithm 1 requires updating π_ω, $\forall \omega \in \Omega$, $\sigma_{\omega,t}$, $\forall \omega \in \Omega, t \in \mathcal{T}$, and $D_{\omega,t,a}$, $\forall \omega \in \Omega, t \in \mathcal{T}, a \in \mathcal{A}$. The values of $C_{\omega,t}$, $\forall \omega \in \Omega, t \in \mathcal{T}$ and $\kappa_{\omega,t,a}$, $\forall \omega \in \Omega, t \in \mathcal{T}, a \in \mathcal{A}$ are constant across each time-step that is simulated by Algorithm 1. The data that are used for this updating are generated and stored in an offline fashion, so that different cases (*i.e.*, with different values of δ or $\kappa_{\omega,t,a}$, $\forall \omega \in \Omega, t \in \mathcal{T}, a \in \mathcal{A}$) use the same underlying data and can be compared to one another directly.

First, we simulate a single sample path of the Markov chains to generate *actual* electricity-supply-disruption and electricity-demand data (*cf.* Sections III-B and III-C). This sample path represents the demands and electricity-supply disruptions that the residential building is modeled as experiencing actually during the 52536 ten-minute time-steps of the case study. Next, for each time-step of the year, we use the Markov chains to generate $|\Omega| = 100$ equiprobable scenarios (*e.g.*, we have $\pi_\omega = 1/|\Omega|$, $\forall \omega \in \Omega$) of forecasted electricity-supply disruptions and demand data during the following 144 ten-minute time-steps. Because demands and electricity-supply disruptions are Markovian, we use the actual demands and electricity-supply disruptions from the first step of the simulation process in generating these scenarios. These sample paths represent probabilistic scenarios that are used by the two-stage stochastic optimization model that is solved in Line 6 of Algorithm 1.

With these two sets of sample paths, the updating in Line 5 of Algorithm 1 is conducted as follows. The values of $\sigma_{\omega,t_{\mathrm{st}}}$, $\forall \omega \in \Omega$ and $D_{\omega,t_{\mathrm{st}},a}$, $\forall \omega \in \Omega, a \in \mathcal{A}$ are set equal to corresponding values from the first sample path. The values of $\sigma_{\omega,t}$, $\forall \omega \in \Omega, t \in \mathcal{T}, t > t_{\mathrm{st}}$, and $D_{\omega,t,a}$, $\forall \omega \in \Omega, t \in \mathcal{T}, t > t_{\mathrm{st}}, a \in \mathcal{A}$ are set equal to corresponding values from the second set of sample paths.

F. Myopic Energy-Storage Use

Our model can exhibit myopic behavior, in that energy storage may not be charged in anticipation of a possible future electricity-supply disruption. The reason for this behavior is that with the small probability of an electricity-supply disruption occurring during any given time-step (*cf.* Section III-C), it is unlikely that any of the $|\Omega| = 100$ scenarios in (1)–(12) predict an electricity-supply disruption. We examine two approaches to mitigate this undesirable myopic behavior.

Under the first approach, which we term scenario augmentation, we select one scenario, $\omega' \in \Omega$, and fix $\sigma_{\omega',t} = 0$, $\forall t \in \mathcal{T}, t > t_{\mathrm{st}}$. We set the value of $\pi_{\omega'}$ to the appropriate value, based on the state-transition probabilities of the Markov chain that governs electricity-supply disruptions. The values of π_ω, $\forall \omega \in \Omega, \omega \neq \omega'$ are fixed equal to:

$$\frac{1 - \pi_{\omega'}}{|\Omega| - 1}.$$

Scenario augmentation yields a scenario that predicts a long-duration electricity-supply disruption (*i.e.*, its duration is the full δ-time-step optimization horizon) that begins during the next time-step. Although the probability of this scenario is minuscule, the high values of $\kappa_{\omega,t,a}$, $\forall \omega \in \Omega, t \in \mathcal{T}, a \in \mathcal{A}$ drive the model to maintain a high energy-storage SOE.

We refer to our second approach to mitigating this myopic behavior as unpreparedness penalization. Under unpreparedness penalization, we add the term:

$$\sum_{\omega\in\Omega,t\in\mathcal{T}} \pi_\omega \Delta K \cdot \left(\bar{E} - E_{\omega,t}\right); \tag{13}$$

to (1), where K is a fixed penalty value. The term (13) imposes a penalty on having the energy-storage SOE below its maximum value. As such, (13) provides a strong incentive to maintain a high energy-storage SOE. The specific value of K is unimportant, so long as it is large relative to $C_{\omega,t}$, $\forall\omega \in \Omega, t \in \mathcal{T}$ (otherwise, the cost of charging energy is higher than the penalty for not having a high energy-storage SOE) and small relative to $\kappa_{\omega,t,a}$, $\forall\omega \in \Omega, t \in \mathcal{T}, a \in \mathcal{A}$ (otherwise, stored energy would not be used to mitigate an *actual* electricity-supply disruption).

Myopic behavior is a common challenge with energy-storage modeling [7]. In its most common form, myopic behavior manifests as energy storage being discharged fully as of the end of the optimization horizon. This behavior arises because with a fixed time horizon, an optimization model does not associate value with keeping stored energy beyond the model horizon. The myopic behavior that we observe manifests differently, but is caused by a similar phenomenon that the model does not ascribe value to having stored energy. There are two commonly used approaches in the literature to address energy storage being discharged fully as of the end of a model horizon. The first is to assign a value to stored energy [44], the second is to constrain the ending SOE of energy storage [45]. The approaches that we examine—scenario augmentation and unpreparedness penalization—can be likened to assigning a value to stored energy.

G. Computational Platform

Our case study is programmed in Python 3.9.1 and uses the PuLP linear-optimization package on a computer with an eight-core 3.80 GHz Intel Core i7-10700k processor and 32 GB of memory. With $\delta = 144$, each instance of (1)–(12) that must be solved in Line 6 of Algorithm 1 has about 259 200 variables and 711 200 constraints. Instances of (1)–(12) with $\delta = 72$ have about half as many variables and constraints.

IV. Case-Study Results

The sample path that gives *actual* power demands and electricity-supply disruptions (*cf.* Section III-E) simulates two disruptions during the course of the year—the first one begins during the second day and the second during the 97th day of the year. We focus our analysis on energy-storage operation before and during the first electricity-supply disruption, which begins during time-step 263 (during 19:40 of 2 January) and ends during time-step 295 (during 1:00 of 3 January). Energy-storage operation is substantively similar during the two electricity-supply disruptions. Energy-storage operation after an electricity-supply disruption is uninteresting, because the important question is whether energy storage is recharged in anticipation of possible future electricity-supply disruptions. Examining operational behavior before the first electricity-supply disruption is indicative of such behavior.

A. Myopic Behavior

Fig. 1 shows actual energy-storage SOE during the first 24 hours of the case study under different variants of the model. The base case includes neither scenario augmentation nor unpreparedness penalties, assumes $\kappa_{\omega,t,a} = 5 \times 10^6$, $\forall\omega \in \Omega, t \in \mathcal{T}$ for high-priority activities (model behavior is the same for other penalty values), and illustrates the aforementioned myopic behavior. The myopic behavior is exhibited by very little energy-storage charging under the base case. This behavior is because during most time-steps, the $|\Omega| = 100$ scenarios in (1)–(12) do not predict an electricity-supply disruption or they predict electricity-supply disruptions far into the future. For instance, when (1)–(12) is solved during time-step 4, four of the scenarios predict electricity-supply disruptions that begin during time-steps 31, 35, 49, and 115. However, the model does not undertake any energy-storage charging during time-step 4, because it anticipates subsequent energy-storage charging before these electricity-supply disruptions occur.

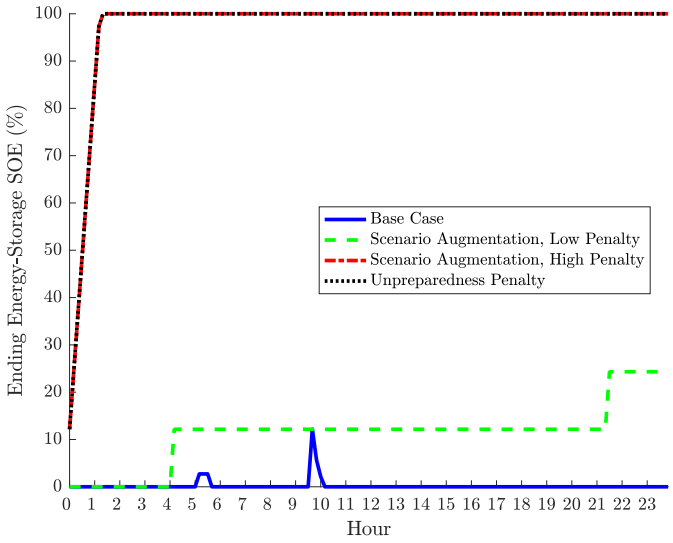

Fig. 1. Ending *actual* energy-storage SOE during first 24 hours of case study with different model variants.

Fig. 1 shows that under the base case the energy storage is charged slightly during time-step 32 and that this charged energy is retained until time-step 35 (there is similar behavior between time-steps 59 and 62). The reason for this behavior is that during time-step 32, one of the scenarios predicts an electricity-supply disruption during time-step 33, which engenders energy-storage charging. Although there are no electricity-supply disruptions during time-steps 33 and 34, the scenario trees during those time-steps predict electricity-supply disruptions during time-steps 34 and 35, respectively. Thus, the model retains the stored energy. The scenario tree during time-step 35 does not predict an electricity-supply disruption during time-step 36. As such, the stored energy is discharged during time-step 35 (to reduce the cost of serving

building energy demand). Overall, the base case that is shown in Fig. 1 shows minimal energy-storage use, due to very few scenarios predicting an electricity-supply disruption during any single time-step.

The remaining cases that are summarized in Fig. 1 correspond to our two approaches to mitigate the myopic behavior that the base case exhibits. We focus first on model performance with scenario augmentation. Energy-storage charging with scenario augmentation depends upon the values of $\kappa_{\omega,t,a}$, $\forall \omega \in \Omega, t \in \mathcal{T}, a \in \mathcal{A}$. Scenario augmentation with low penalties ($\kappa_{\omega,t,a} = 2 \times 10^6$, $\forall \omega \in \Omega, t \in \mathcal{T}$ for high-priority activities) yields some, but limited energy-storage charging. The reason for this behavior is that the small probability of the augmented scenario outweighs the relatively low penalties for unserved demand. Scenario augmentation with high penalties ($\kappa_{\omega,t,a} = 5 \times 10^6$, $\forall \omega \in \Omega, t \in \mathcal{T}$ for high-priority activities, although energy-storage charging is identical for higher penalty values) yields nearly immediate energy-storage charging. The final case that is summarized in Fig. 1 assumes unpreparedness penalties and yields the same immediate energy-storage charging that is observed with scenario augmentation with high penalties. Thus, so long as the values of $\kappa_{\omega,t,a}$, $\forall \omega \in \Omega, t \in \mathcal{T}, a \in \mathcal{A}$ are sufficiently high, scenario augmentation yields the same behavior between electricity-supply disruptions that unpreparedness penalties do.

B. Energy Use During an Electricity-Supply Disruption

Fig. 2 shows actual energy-storage SOE during the course of the electricity-supply disruption that begins as of 19:40 during 2 January, with different penalty values for high-priority activities and using scenario augmentation or unpreparedness penalties. Fig. 3 shows corresponding cumulative curtailment of energy for low-priority activities. Figs. 2 and 3 show that setting higher penalty values for high-priority activities tends to yield more conservative energy-storage use, as does the unpreparedness penalty. The fundamental trade-off during an electricity-supply disruption is how much energy to use during the current time-step as opposed to how much to retain for future energy needs, especially if the disruption is realized as having a prolonged duration.

If the penalty values for high- and low-priority activities are close to one another, there is relatively little benefit in storing energy for future energy needs. As such, energy tends to be used earlier during an electricity-supply disruption, which reduces the energy-storage SOE and may yield subsequent curtailment of high-priority activities if the electricity-supply disruption has a long duration. This exact outcome is shown in Figs. 2 and 3. The low-penalty cases result in the battery being depleted of energy before the electricity-supply disruption ends (this is exacerbated with scenario augmentation, because as Fig. 1 shows, the battery is not charged fully before the disruption begins). As such, there is less curtailment of low-priority activities (relative to the high-penalty cases) under the low-penalty case with unpreparedness penalties early during the electricity-supply disruption. However, this aggressive use of stored energy results in 1.2 kWh of energy demand for high-priority activities being curtailed under the low-penalty case

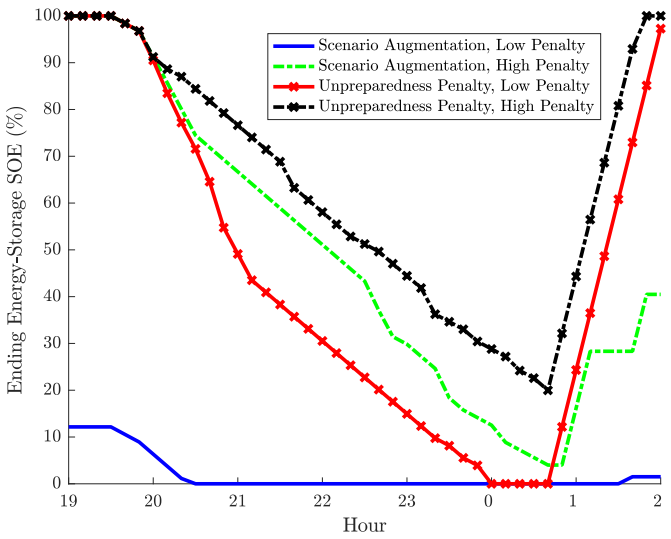

Fig. 2. Ending *actual* energy-storage SOE during electricity-supply disruption with different penalty values for high-priority activities and using scenario augmentation or unpreparedness penalties.

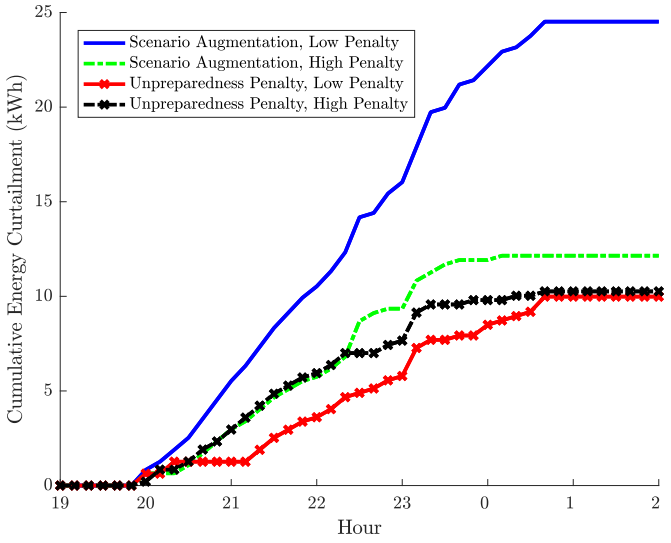

Fig. 3. Cumulative energy curtailment for low-priority activities during electricity-supply disruption with different penalty values for high-priority activities and using scenario augmentation or unpreparedness penalties.

with unpreparedness penalties. Conversely, no high-priority activities are curtailed under the high-penalty cases.

The high-penalty case yields much more conservative energy use compared to the low-penalty cases. There is some stored energy in the battery as of the end of the electricity-supply disruption under the high-penalty cases. Thus, for this particular electricity-supply disruption, the behavior under the high-penalty case is 'too conservative' insomuch as some stored energy could have been used (with hindsight) to reduce earlier curtailment of low-penalty activities.

C. Optimization Horizon

Fig. 4 shows cumulative energy curtailment with scenario augmentation, $\kappa_{\omega,t,a} = 5 \times 10^6$, $\forall \omega \in \Omega, t \in \mathcal{T}$ for high-priority activities, and $\delta = 144$ or 72 in Algorithm 1. The

results are qualitatively similar with unpreparedness penalties. Having $\delta = 72$ as opposed to $\delta = 144$ reduces the size of (1)–(12) roughly in half, which cuts solution time from about 30 s with $\delta = 144$ to about 10 s with $\delta = 72$. Algorithm 1 requires solving (1)–(12) 52536 times to simulate the operation of the battery over the course of year. Thus, total time to implement Algorithm 1 across the case-study year is about 438 h with $\delta = 144$ and 146 h with $\delta = 72$. Moreover, if energy storage is to be used in this way in practice, a model that is akin to (1)–(12) must be implemented to optimize energy-storage charging and discharging. Simplifying (1)–(12) reduces the requisite hardware and software.

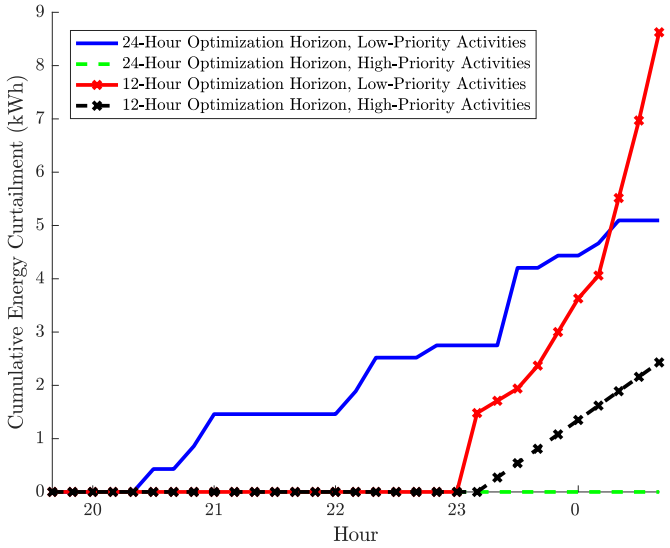

Fig. 4. Cumulative energy curtailment during electricity-supply disruption with different optimization horizons and scenario augmentation.

Having $\delta = 144$ or 72 yields differences in how energy storage is used during an electricity-supply disruption. Battery charging between disruptions is not affected by the value of δ. Having $\delta = 72$ gives the model a shorter optimization horizon when determining how to use stored energy (*e.g.*, how much to use to serve current demands as opposed to save to serve future demands). The longer optimization horizon with $\delta = 144$ results in demand for low-priority activities being curtailed earlier than happens with $\delta = 72$. This curtailed demand for low-priority activities with $\delta = 144$ means that demand for high-priority activities are not curtailed during the electricity-supply disruption. Conversely, with $\delta = 72$, more low-priority demands are served earlier during the electricity-supply disruption. As such, eventually demands for both low- and high-priority activities must be curtailed, once the energy-storage SOE is sufficiently low.

V. Conclusions

This paper examines the use of on-site energy storage to provide electricity service to a residential customer during electricity-supply disruptions. The resultant increase in electricity-service resilience and reliability may be beneficial if a customer has sensitive electricity demands (*e.g.*, refrigerating food) or unacceptably unreliable electricity service. Our model allows stored energy to be used, considering uncertain future electricity-supply disruptions (when they occur and their durations) and power demands. We develop a rolling-horizon algorithm that can be used to operate the energy storage in real-time, as system conditions and forecasts of future system conditions evolve. The algorithm is computationally efficient using standard computing hardware and off-the-shelf optimization software. Thus, our model could be used in a building-energy-management system to manage a battery as part of a real-world deployment.

We demonstrate the model and algorithm using a case study that is calibrated to real-world data for AEP Ohio's Central-Ohio service territory. We demonstrate that with the low probability of an energy-service disruption occurring during any given ten-minute time-step, the small scenario tree that we use in our model does not incentivize energy-storage charging. We use scenario augmentation and unpreparedness penalties as ways to overcome this undesirable myopic behavior. During an electricity-supply disruption, there is a trade-off between using stored energy immediately or saving it for subsequent use. Depending upon the conservatism of the model, which is controlled by the penalty values, the model may be overly or under conservative in using stored energy.

We abstract away the physical details of the energy-storage medium. Our case study assumes implicitly that the energy storage is a stationary system (a Tesla Powerwall would be an example of such a commercial product). However, there may be other options for the energy-storage medium. One possibility is to use the on-board battery of an electric vehicle (EV), which would have the cost advantage that it would not necessitate the purchase of a dedicated battery solely for backup energy. Using an EV battery in this manner would require trading-off between using stored energy for building as opposed to transportation energy demands. Moreover, such a use of an EV battery can exacerbate cycle-life loss and damage, which may be detrimental for electromobility. On the other hand, an EV battery could allow for mobile stored energy. For instance, an EV can be driven and connect to another area of the electricity system that has energy supply and return to the residential building with stored energy. Given these and other considerations, such uses of EV batteries represent a vast and interesting area for further study.

Our case study assumes that the *desired* activities of the building occupants (and the associated electricity demands) remain the same when the building experiences an electricity-supply disruption as they would be in its absence. This is a reasonable assumption, because Lee and Akar [43] do not report findings that residential consumers have significantly different energy-use desires during versus absent an electricity-supply disruption. However, there could be instances in which some residential consumers' energy demands differ with as opposed to without an electricity-supply disruption. Studying such a case is beyond the scope of our case study, but our model and algorithm could be employed to study such a situation.

Our work focuses solely on the feasibility and resultant operation of using energy storage to mitigate electricity-supply disruptions. An important related question is the cost of

deploying such a solution relative to a residential customer's willingness and ability to pay for it. Such an analysis is beyond the scope of our work. Ultimately, such a cost-benefit analysis is highly sensitive to consumer willingness to pay. Unfortunately, the data that are provided to us by Lee and Akar [43] are limited in being able to answer such a question. This is because the Lee and Akar study examines the relative importance of different electricity uses during a supply disruption. Their study does *not* provide robust estimates of the absolute willingess to pay of the survey respondents. Nonetheless, this is a fruitful area for future research.

ACKNOWLEDGMENT

The authors thank A. Sorooshian, the editors, and three reviewers for helpful discussions, suggestions, and comments. Any remaining errors are entirely those of the authors.

REFERENCES

[1] J. Doss-Gollin, D. J. Farnham, U. Lall, and V. Modi, "How unprecedented was the February 2021 Texas cold snap?" *Environmental Research Letters*, vol. 16, p. 064056, June 2021.

[2] K. H. LaCommare and J. H. Eto, "Understanding the Cost of Power Interruptions to U.S. Electricity Consumers," Ernest Orlando Lawrence Berkeley National Laboratory, Berkeley, CA, Tech. Rep. LBNL-55718, September 2004.

[3] A. Bhattacharyya, S. Yoon, and M. Hastak, "Economic Impact Assessment of Severe Weather-Induced Power Outages in the US," *Journal of Infrastructure Systems*, vol. 27, p. 04021038, December 2021.

[4] S. Stoft, *Power System Economics: Designing Markets for Electricity*. New York, New York: Wiley-Interscience, 2002.

[5] C. von Hirschhausen, T. Beckers, and A. Brenck, "Infrastructure regulation and investment for the long-term—an introduction," *Utilities Policy*, vol. 12, pp. 203–210, December 2004.

[6] P. Balducci, K. Mongird, and M. Weimar, "Understanding the Value of Energy Storage for Power System Reliability and Resilience Applications," *Current Sustainable/Renewable Energy Reports*, vol. 8, pp. 131–137, September 2021.

[7] R. Sioshansi, P. Denholm, J. Arteaga, S. Awara, S. Bhattacharjee, A. Botterud, W. Cole, A. Cortés, A. de Queiroz, J. DeCarolis, Z. Ding, N. DiOrio, Y. Dvorkin, U. Helman, J. X. Johnson, I. Konstantelos, T. Mai, H. Pandžić, D. Sodano, G. Stephen, A. Svoboda, H. Zareipour, and Z. Zhang, "Energy-Storage Modeling: State-of-the-Art and Future Research Directions," *IEEE Transactions on Power Systems*, vol. 37, pp. 860–875, March 2022.

[8] R. Perez, M. Taylor, T. Hoff, and J. P. Ross, "Reaching Consensus in the Definition of Photovoltaics Capacity Credit in the USA: A Practical Application of Satellite-Derived Solar Resource Data," *IEEE Journal of Selected Topics in Applied Earth Observations and Remote Sensing*, vol. 1, pp. 28–33, March 2008.

[9] S. H. Madaeni, R. Sioshansi, and P. Denholm, "Estimating the Capacity Value of Concentrating Solar Power Plants with Thermal Energy Storage: A Case Study of the Southwestern United States," *IEEE Transactions on Power Systems*, vol. 28, pp. 1205–1215, May 2013.

[10] P. Denholm, J. Nunemaker, P. Gagnon, and W. Cole, "The Potential for Battery Energy Storage to Provide Peaking Capacity in the United States," National Renewable Energy Laboratory, Golden, CO, Tech. Rep. NREL/TP-6A20-74184, June 2019.

[11] B. Klöckl and G. Papaefthymiou, "An effort to overcome the chronological modeling methods for energy storage devices," in *2005 International Conference on Future Power Systems*. Amsterdam, Netherlands: Institute of Electrical and Electronics Engineers, 18 November 2005.

[12] R. Sioshansi, S. H. Madaeni, and P. Denholm, "A Dynamic Programming Approach to Estimate the Capacity Value of Energy Storage," *IEEE Transactions on Power Systems*, vol. 29, pp. 395–403, January 2014.

[13] G. Edwards, S. Sheehy, C. J. Dent, and M. C. M. Troffaes, "Assessing the contribution of nightly rechargeable grid-scale storage to generation capacity adequacy," *Sustainable Energy, Grids and Networks*, vol. 12, pp. 69–81, December 2017.

[14] H. J. Kim, R. Sioshansi, E. Lannoye, and E. Ela, "A Stochastic-Dynamic-Optimization Approach to Estimating the Capacity Value of Energy Storage," *IEEE Transactions on Power Systems*, vol. 37, pp. 1809–1819, May 2022.

[15] B. Bagen and R. Billinton, "Impacts of Energy Storage on Power System Reliability Performance," in *2005 Canadian Conference on Electrical and Computer Engineering*. Saskatoon, Saskatchewan, Canada: Institute of Electrical and Electronics Engineers, 1-4 May 2005, pp. 494–497.

[16] P. Hu, R. Karki, and R. Billinton, "Reliability evaluation of generating systems containing wind power and energy storage," *IET Generation, Transmission & Distribution*, vol. 3, pp. 783–791, August 2009.

[17] L. H. Koh, G. Z. Yong, W. Peng, and K. J. Tseng, "Impact of Energy Storage and Variability of PV on Power System Reliability," *Energy Procedia*, vol. 33, pp. 302–310, 2013.

[18] Y. Zhou, P. Mancarella, and J. Mutale, "Framework for capacity credit assessment of electrical energy storage and demand response," *IET Generation, Transmission & Distribution*, vol. 10, pp. 2267–2276, 9 June 2016.

[19] I. Konstantelos, P. Djapic, G. Strbac, P. Papadopoulos, and A. Laguna, "Contribution of energy storage and demand-side response to security of distribution networks," *CIRED - Open Access Proceedings Journal*, vol. 2017, pp. 1650–1654, October 2017.

[20] G. Stephen, "Probabilistic Resource Adequacy Suite (PRAS) v0.6 Model Documentation," National Renewable Energy Laboratory, Golden, CO, Tech. Rep. NREL/TP-5C00-79698, May 2021.

[21] R. Moreno, R. Moreira, and G. Strbac, "A MILP model for optimising multi-service portfolios of distributed energy storage," *Applied Energy*, vol. 137, pp. 554–566, 1 January 2015.

[22] M. A. Mansouri and R. Sioshansi, "The Effect of Natural-Gas Prices on Power-System Reliability," *Current Sustainable/Renewable Energy Reports*, vol. 8, pp. 164–173, September 2021.

[23] B. Zhang, D. Stenclik, and W. Hall, "Calculating the Capacity Value and Resource Adequacy of Energy Storage on High Solar Grids," in *2018 Grid of the Future*, no. 2018-18. Reston, VA: Conseil International des Grands Réseaux Électriques, 28-31 October 2018.

[24] K. Parks, "Declining Capacity Credit for Energy Storage and Demand Response With Increased Penetration," *IEEE Transactions on Power Systems*, vol. 34, pp. 4542–4546, November 2019.

[25] K. Carden and N. Wintermantel, "Energy Storage Capacity Value on the CAISO System," Astrapé Consulting, Tech. Rep., 20 November 2019.

[26] D. Sodano, J. F. DeCarolis, A. Rodrigo de Queiroz, and J. X. Johnson, "The symbiotic relationship of solar power and energy storage in providing capacity value," *Renewable Energy*, vol. 177, pp. 823–832, November 2021.

[27] R. Sioshansi and P. Denholm, "The Value of Concentrating Solar Power and Thermal Energy Storage," *IEEE Transactions on Sustainable Energy*, vol. 1, pp. 173–183, October 2010.

[28] S. H. Madaeni, R. Sioshansi, and P. Denholm, "How Thermal Energy Storage Enhances the Economic Viability of Concentrating Solar Power," *Proceedings of the IEEE*, vol. 100, pp. 335–347, February 2012.

[29] P. Denholm and T. Mai, "Timescales of Energy Storage Needed for Reducing Renewable Energy Curtailment," National Renewable Energy Laboratory, Golden, CO, Tech. Rep. NREL/TP-6A20-68960, September 2017.

[30] L. L. Garver, "Effective Load Carrying Capability of Generating Units," *IEEE Transactions on Power Apparatus and Systems*, vol. PAS-85, pp. 910–919, August 1966.

[31] R. Billinton and R. N. Allan, *Reliability Evaluation of Power Systems*. Boston, Massachusetts: Pitman Advanced Publishing Program, 1984.

[32] R. Billinton and P. Wang, "Distribution System Reliability Cost/Worth Analysis Using Analytical and Sequential Simulation Techniques," *IEEE Transactions on Power Systems*, vol. 13, pp. 1245–1250, November 1998.

[33] X. Xi, R. Sioshansi, and V. Marano, "A Stochastic Dynamic Programming Model for Co-optimization of Distributed Energy Storage," *Energy Systems*, vol. 5, pp. 475–505, September 2014.

[34] O. Mégel, J. L. Mathieu, and G. Andersson, "Scheduling distributed energy storage units to provide multiple services under forecast error," *International Journal of Electrical Power & Energy Systems*, vol. 72, pp. 48–57, November 2015.

[35] X. Xi and R. Sioshansi, "A Dynamic Programming Model of Energy Storage and Transformer Deployments to Relieve Distribution Constraints," *Computational Management Science*, vol. 13, pp. 119–146, January 2016.

[36] D. Metz and J. T. Saraiva, "Simultaneous co-integration of multiple electrical storage applications in a consumer setting," *Energy*, vol. 143, pp. 202–211, 15 January 2018.
[37] S. Varghese and R. Sioshansi, "The Price is Right? How Pricing and Incentive Mechanisms in California Incentivize Building Distributed Hybrid Solar and Energy-Storage Systems," *Energy Policy*, vol. 138, p. 111242, March 2020.
[38] J. Jin, L. Hao, Y. Xu, J. Wu, and Q.-S. Jia, "Joint Scheduling of Deferrable Demand and Storage With Random Supply and Processing Rate Limits," *IEEE Transactions on Automatic Control*, vol. 66, pp. 5506–5513, November 2021.
[39] E. A. Martínez Ceseña, N. Good, A. L. A. Syrri, and P. Mancarella, "Techno-economic and business case assessment of multi-energy microgrids with co-optimization of energy, reserve and reliability services," *Applied Energy*, vol. 210, pp. 896–913, 15 January 2018.
[40] J. R. Birge and F. Louveaux, *Introduction to Stochastic Programming*, corrected ed. New York, New York: Springer Verlag, 1997.
[41] M. Muratori, M. C. Roberts, R. Sioshansi, V. Marano, and G. Rizzoni, "A highly resolved modeling technique to simulate residential power demand," *Applied Energy*, vol. 107, pp. 465–473, July 2013.
[42] M. Muratori, V. Marano, R. Sioshansi, and G. Rizzoni, "Energy consumption of residential HVAC systems: a simple physically-based model," in *2012 IEEE Power and Energy Society General Meeting*. San Diego, CA, USA: Institute of Electrical and Electronics Engineers, 22-26 July 2012.
[43] J. Y. Lee and G. Akar, "Electric Vehicles, Power outages and Willingness to pay," in *58th Annual ACSP Conference*. Buffalo, NY: Association of Collegiate Schools of Planning, 25-28 October 2018.
[44] R. Sioshansi, "Optimized Offers for Cascaded Hydroelectric Generators in a Market with Centralized Dispatch," *IEEE Transactions on Power Systems*, vol. 30, pp. 773–783, March 2015.
[45] F. Graves, T. Jenkin, and D. Murphy, "Opportunities for Electricity Storage in Deregulating Markets," *The Electricity Journal*, vol. 12, pp. 46–56, October 1999.

Rachel Hunter-Rinderle holds the B.S. and M.S. degrees in industrial and systems engineering, both from The Ohio State University, Columbus, OH USA.

Matthew Y. Fong (S'23) is pursuing a B.S. degree in computer science and engineering from The Ohio State University, Columbus, OH, USA, while working in cybersecurity with event-log data.

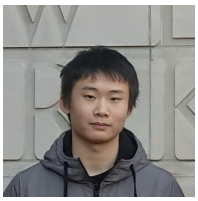

Baihua Yang holds the B.S. degree in computer and information science from The Ohio State University, Columbus, OH, USA. He is currently an M.S. student in computer science in Viterbi School of Engineering at University of Southern California, Los Angeles, CA, USA.

Haoshu Xian holds the B.S. degree in industrial and system engineering from The Ohio State University, Columbus, OH, USA and the B.E. degree in industrial engineering from Sichuan University, Chengdu, Sichuan, China.

He is an M.S.E. student in Department of Industrial and Operations Engineering at University of Michigan, Ann Arbor, Ann Arbor, MI, USA. His research focuses on energy-system analysis, quality control, and warehouse-facility layout.

Ramteen Sioshansi (M'11–SM'12–F'21) holds the B.A. degree in economics and applied mathematics and the M.S. and Ph.D. degrees in industrial engineering and operations research from University of California, Berkeley, Berkeley, CA, USA and an M.Sc. in econometrics and mathematical economics from London School of Economics and Political Science, London, U.K.

He is a professor in Department of Engineering and Public Policy and Department of Electrical and Computer Engineering, Director of Carnegie Mellon Electricity Industry Center, and a faculty affiliate of Wilton E. Scott Institute for Energy Innovation at Carnegie Mellon University, Pittsburgh, PA, USA and an adjunct professor in Department of Integrated Systems Engineering at The Ohio State University, Columbus, OH, USA. His research focuses on analyzing renewable and sustainable energy systems and the design of restructured competitive electricity markets.